Salinity gradient energy conversion by custom-made interpolymer ion exchange membranes utilized in reverse electrodialysis system*

Esra Altıok[1], Tuğçe Zeynep Kaya[1], Katarzyna Smolinska-Kempisty[2], Enver Güler[3], Nalan Kabay[1*], Barbara Tomaszewska[4], Marek Bryjak[2*]

[1]Ege University, Faculty of Engineering, Chemical Engineering Department, 35100 Izmir, Turkey
[2]Wroclaw University of Technology, Faculty of Chemistry, Department of Process Engineering and Technology of Polymer and Carbon Materials, 50-370 Wroclaw, Poland
[3]Atılım University, Faculty of Engineering, Department of Chemical Engineering, 06830 Ankara, Turkey
[4]AGH University of Science and Technology, Faculty of Geology, Geophysics and Environmental Protection Department of Fossil Fuels, 30-059 Cracow, Poland

Abstract

Reverse electrodialysis (RED) is one of methods to extract salinity gradient energy between two aqueous solutions with different salt concentrations. In this work, custom-made interpolymer ion exchange membranes were employed in the RED stack. The effects of divalent (Mg^{2+}, Ca^{2+} and SO_4^{2-}) and monovalent (Li^+, K^+ and Cl^-) ions in the feed solutions prepared from NaCl salt as a function of such process parameters as number of membrane pairs, flow rate, and salinity ratio on power generation by the RED method were studied. It was shown that the maximum power density of 0.561 W/m^2 was reached by using three membrane pairs using 1:45 of salt ratio with a feed flow rate of 120 mL/min using only NaCl salt in the feed solutions. The maximum power density was 0.398 W/m^2 at 120 mL/min of the flow rate of the feed solutions composed of 90 wt% NaCl and 10 wt% KCl by using a salt ratio of 1:30 while the lowest power density of 0.246 W/m^2 was obtained with a feed flow rate of 30 mL/min in the presence of SO_4^{2-} ions with a similar salt ratio. Consequently, it was seen that while the presence of divalent ions in NaCl solutions had negative impact on power generation by RED system, the addition of monovalent ions having smaller hydrated radius than that of the Na^+ ions contributed positively to the power generation.

Keywords: Blue energy, interpolymer ion exchange membrane, reverse electrodialysis (RED), salinity gradient energy.

Corresponding authors:

N.Kabay (nalan.kabay@ege.edu.tr) & M.Bryjak (marek.bryjak@pwr.edu.pl)

*Published by Journal of Environmental Chemical Engineering, https://doi.org/10.1016/j.jece.2023.109386

1. Introduction

The production of energy at a sufficient level is one of the major requirements of daily life. Nowadays, energy utilization having its wide usage spots is an inevitable part of our social and economic activities. Especially for urban life, the rates of energy production and consumption are the primary development criteria used to determine social and economic progresses. The world's energy demand is largely met by fossil fuels usage, and this resulted in climate changes. Unless a solution for this situation is found, the ecosystem will be deteriorated, thus some plant and animal species will disappear by time.

The concern about possible negative consequences arising from the usage of fossil fuels has increased the interest in clean energy production [1]. The investigations tend to renewable and green energy sources such as hydroelectric, wind, solar, geothermal, biomass, hydrogen, and salinity gradient energies. In addition, some renewable energy sources offered by oceans are winds, waves, tides, and salinity gradient which is known as “blue energy” [2-4].

The Gibbs free energy that occurred from the controlled mixing of solutions having different salt concentrations can be utilized for providing a major part of energy demand [1-5]. In the literature, it was reported that there is a great potential to obtain a power of 2 TW from the salinity gradient [6-8].

Selective transport of anions to the anode through the anion exchange membranes (AEMs) and cations towards cathode by means of cation exchange membranes (CEMs) occur in the RED process [9-11]. In 1954, Pattle performed the initial studies about the RED method and demonstrated that energy generation can be achieved by mixing two solutions having different salinities [12]. According to the literature, increasing flow rate of the feed solutions resulted in an increase in power generation [13, 14]. The optimization of the process parameters is the most important issue in terms of the application of this technique in the industry. For this purpose, some studies to see the effect of such process variables as flow rate and salinities of feed solutions were carried out. Lacey [15] reported that the ion exchange membranes (IEMs) having lower electrical resistance and higher selectivity should be used to enhance the power to be generated from the RED stack. Increasing the feed flow rate resulted in a positive effect on hydrodynamic mixing and let a facile transfer of ions through the IEMs in the RED stack by improving the potential difference across the membranes and thus enhancing the power density to be obtained [16].

Zoungrana and Cakmakci investigated the effect of salinity ratio and flow rate of feed solutions on the performance of a RED system [17]. Except the salt concentration in high

*Published by Journal of Environmental Chemical Engineering, https://doi.org/10.1016/j.jece.2023.109386

saline solution, the other parameters such as salt concentration in low saline solution and feed flow rate were kept constant in that study. They observed that an increase in power density from 0.345 to 0.705 W/m^2 was achieved with increasing salt (NaCl) concentration in high saline solution from 171 mM to 686 mM, respectively. In the same study, effect of the flow rate of feed solutions was also analyzed by using five different feed flow rates (15, 30, 45, 60 and 75 mL/min). It was concluded that increasing the feed flow rate up to 60 mL/min resulted in a maximum power density of 0.540 W/m^2 by the RED system [17].

The IEMs produced for electromembrane systems are generally used for the ED process. Lack of RED-specific membranes, high production costs, and the relatively lower power densities generated by currently available IEMs are the main problems limiting their uses in the RED systems. Custom-made IEMs for RED studies were designed to have appropriate chemical and physical properties, high permselectivity, low resistance, mechanical durability along with straightforward and environmentally friendly synthesis routes [18,19].

In a case of IEMs used for RED tests, there are basically two dominating features in RED performance: permselectivity and electrical resistance. Membrane characteristics such as water content and ion exchange capacity could affect energy production through permselectivity and membrane resistance. A high water content in IEMs causes some decline in mechanical stability and permselectivity. However, it favorably reduces the membrane resistance. Thus, the proper selection of these two properties is critical for power output performances of the RED system. Another membrane feature that affects energy generation is the structure of IEMs. Generally, two types of IEMs as homogeneous and heterogeneous membranes are available. In the first case, the membrane matrix is uniformly charged while in the second case a membrane contains an uncharged binder that makes a non-uniform charge distribution. Usually, the heterogeneous membranes are thicker than the homogenous ones and in consequence they have higher resistances [20].

Another important property of IEMs to be used for RED studies is their selectivity for the monovalent ions. Monovalent selective membranes facilitate transport of ions having single charge and block the transfer of multivalent ions. According to the literature [21], this property has been shown to be critical for power generation by RED.

In recent years, for the improvement of the power generation of a RED system by using natural water sources like seawater and river water, some investigations has been performed in the presence of co-existing ions in natural water sources. Vermaas et al. [22] studied the impact of multivalent ions on power generation by using different types of IEMs such as

heterogeneous Ralex CMH & AMH and homogeneous Neosepta CMX & AMX, Fujifilm V1 membranes in the RED system. In the feed streams having high and low salt concentrations, NaCl has been mixed with $MgSO_4$, $MgCl_2$, or Na_2SO_4 by keeping the salt ratio constant as 1:30 (g salt in low saline solution/g salt in high saline solution). Elsewhere, Guo et al. [23] studied the effects of the temperature and co-existing ions such as SO_4^{2-}, Ca^{2+}, Mg^{2+}, and K^+ on the RED performance. At the end of the experimental study, the positive influence of temperature and the negative effect of co-existing ions on RED performance were obtained. It was reported that the power density and open circuit voltage (OCV) decreased whereas the electrical resistance increased in the presence of Mg^{2+} and SO_4^{2-} ions in the feed solution. Pintossi [24] has calculated the electrical resistance of the CEMs and explained the increase in the electrical resistance of CEMs related to the interaction between ions in the feed streams and functional groups on the membrane structure. Furthermore, the effects of divalent cations on the performance of the monovalent selective Neosepta CMS membranes and multivalent-permeable Fuji T1 membranes were investigated by Rijnaarts et al. [25]. They compared the results obtained with the performance of the standard grade CEMs. Oh et al. [26] investigated the impact of the divalent cations (Ba^{2+}, Ca^{2+}, and Mg^{2+}) on the electrical resistance of IEMs (Fujifilm Type 1 AEM, and Fujifilm Type 1 CEM) used for power generation by the RED system. Because of the strong affinity of Mg^{2+} ions toward the fixed functional groups in CEMs, the ionic mobilities of Mg^{2+} ions were reduced and therefore, the electrical resistances of the CEMs increased. It was observed that the normalized OCV and the normalized maximum power density decreased with the addition of Mg^{2+}or Ca^{2+} ions.

In this study, RED tests were carried out using custom-made interpolymer IEMs. The influences of such operational parameters as the number of membrane pairs, feed flow rate, and salt ratio between low saline and high saline solutions on power generation by RED were studied. Additionally, the effects of divalent (Mg^{2+}, Ca^{2+} and SO_4^{2-}) and monovalent (Li^+, K^+ and Cl^-) ions in the feed solutions (NaCl solutions) on the performance of the RED system were investigated.

2. Experimental

2.1 Synthesis of custom-made interpolymer IEMs

The interpolymer IEMs were synthesized by modification of polyethylene (PE)//styrene-co-divinylbenzene (DVB) interpolymer films as reported before [25]. For this, PE pellets have been swollen with a mixture of styrene and DVB along with benzoyl peroxide (BPO) as the

*Published by Journal of Environmental Chemical Engineering, https://doi.org/10.1016/j.jece.2023.109386

radical initiator. Polymerization of styrene and DVB in PE pellets has been done at 90°C for 3 h. The PE//styrene-co-DVB interpolymer was composed of 30% wt. of styrene, 68%wt. of PE, and 2%wt. of DVB. Homogenization of interpolymer was done in an extruder at 120°C. Chlorosulfonation of interpolymers was carried out by placing the extruded films in a mixture of chlorosulfonic acid in dichloroethane (15:35 vol:vol) and kept there for 1 h at room temperature. After this time, they were immersed in dioxane for 30 min and washed with methanol. The reaction was stopped by submerging membranes in dioxane for 30 min and washing them with methanol. For production of CM-KESD, the chlorosulfonated membranes were kept in 20% (w/w) of NaOH solution for 24 h at room temperature. In the case of CM-AESD, the chlorosulfonated membranes were placed in 50% of ethylenediamine solution in mixture of water and methanol (1:1) for 24 h at room temperature. Finally, the membranes were dipped alternately in 1 M HCl and 1 M NaOH solutions. As the last step, both CM-AESD and CM-KESD membranes were washed with large volume of water [27]. Some properties of the interpolymer IEMs synthesized were summarized in Table 1. The images of these custom-made IEMs are shown in Figure 1. Prior to use, these IEMs were soaked in 0.5 M of NaCl solution overnight.

Table 1. Some properties of custom-made interpolymer IEMs [27, 28]

IEMs		**CM-AESD**	**CM-KESD**
Composition		%30 Styrene, %68 PE, %2 DVB	
Thickness (µm)		200 ± 5	211 ± 5
Ion exchange capacity (mmol/g)		0.80 ± 0.06	1.03 ± 0.010
Permselectivity (%)		88.3 ± 2.3	92.6 ± 0.5
Area Resistance (Ω cm^2)		0.95 ± 0.04	4.22 ± 0.30
Swelling degree (%)		20.3 ± 0.6	38.1 ± 0.9
Surface Tension (mJ/m)		41.5±0.2	46.5±0.2
Contact angles (º)	**water**	64.5 ± 2	70.5 ± 6
	formamide	53.1 ± 4.5	54.6 ± 7
	diiodomethane	37.7 ± 5	36.6 ± 5.5

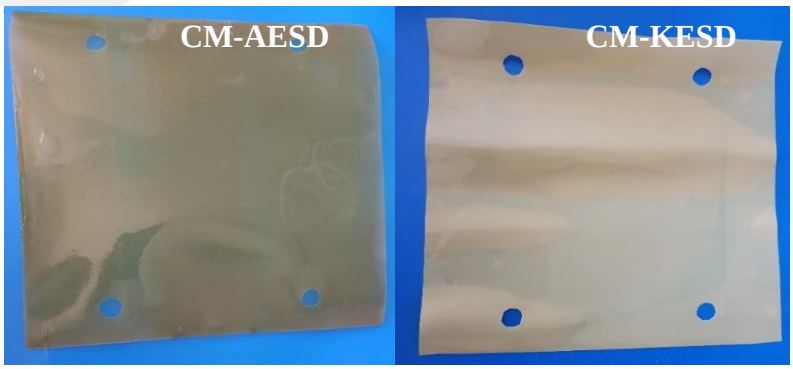

*Published by Journal of Environmental Chemical Engineering, https://doi.org/10.1016/j.jece.2023.109386

Figure 1. The images of CM-AESD and CM-KESD membranes

2.2 RED Tests

A lab-scale RED system having 10 cm × 10 cm of electrode area was employed for the tests. The RED system set-up (RED stack from STT Products B.V., The Netherlands) consists of two feed tanks (LSS: low-salt solution and HSS: high-salt solution), an electrode solution tank, and peristaltic pumps to feed the solutions into the membrane stack. The inner arrangement of RED membrane stack is formed by placing polyamide mesh spacer and silicone gaskets (totally 400 μm thick) between the sequential pairs of CEMs and AEMs membranes. The scheme of the RED system is shown in Figure 2.

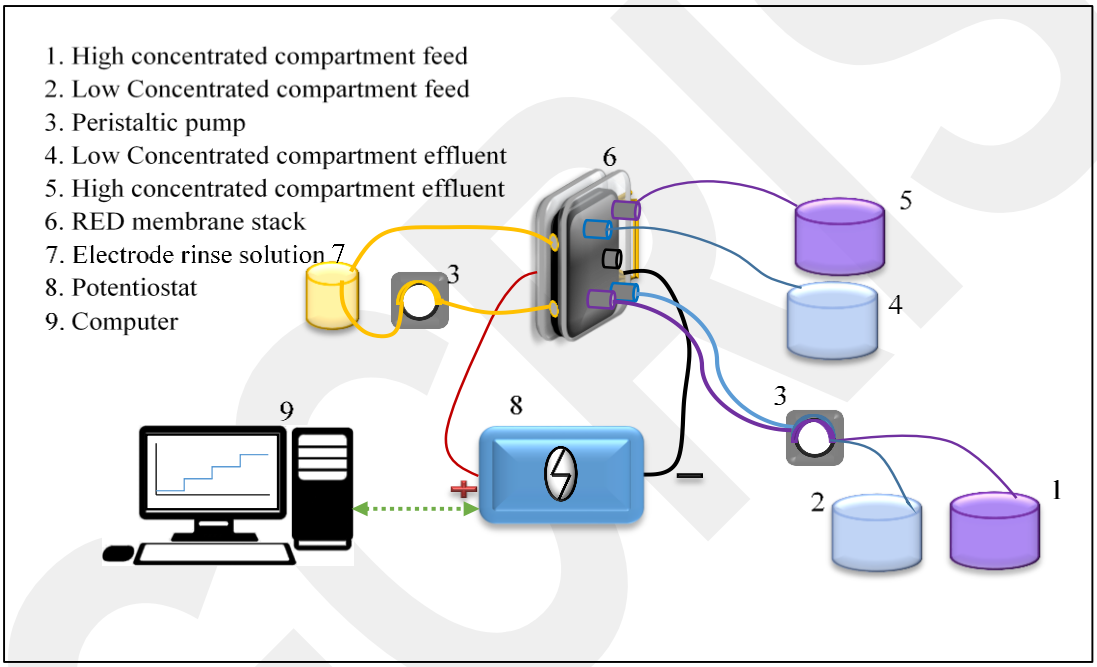

Figure 2. Flowsheet of the RED system

The electrode solution is a mixture containing 0.05 M of $K_3[Fe(CN)_6]$, 0.05 M of $K_4[Fe(CN)_6]\cdot 3H_2O$ and 0.25 M of NaCl. This solution was circulated in the electrode compartments at a 300 mL/min of flow rate.

In order to ensure a regular flow in the cell, the system was kept waiting for 5 min before the data were collected. The given results are based on the averages of three tests results. For blank tests and RED calculations, similar procedures were followed as reported before [11].

The potentiostat (Gamry Instruments Reference 3000, USA) was used for monitoring the electrochemical measurements. The chronopotentiometry method was applied for monitoring the open circuit voltage and current–voltage relation results. The voltage value measured at

*Published by Journal of Environmental Chemical Engineering, https://doi.org/10.1016/j.jece.2023.109386

zero current yields the maximum voltage value, which is referred to as the open circuit voltage (OCV). By multiplying the current (I) with the potential difference (V), the electrical power (W) generated by the RED system was calculated (Equation (1)) [11].

$$W = V \cdot I \quad (1)$$

P_{gross}, the gross power density (W/m^2), was calculated by the power divided by the total active membrane area (m^2) where W is power (W), A is an effective membrane area of only one membrane (m^2) and N is the number of membrane using Equation (2) [11].

$$P_{gross} = \frac{W}{2A \cdot N} \quad (2)$$

2.2 RED tests with only NaCl solutions

In this part, the RED studies were performed to investigate the effect of some operational parameters on the RED performance by using two different salt solutions (NaCl solutions) specified as low saline solution (LSS) and high saline solution (HSS) prepared using different salt (NaCl) concentrations. With these salt solutions, the effects of membrane pair number, salt ratio, and feed flow rates on OCV, power density, and power produced in the RED system were investigated. The number of membrane pair was 2 or 3. The salt ratios (S) were changed as 1:15, 1:30 and 1:45 (g NaCl in LSS : g NaCl in HSS) while applying four different feed flow rates adapted according to number of membrane pairs (Table 2). Salinity measurement was performed with a portable conductometer (WTW Conductometer 3110 model).

Table 2. Operational conditions for studies with only NaCl solutions

IEMs	CM-AESD and CM-KESD
Numbers of membrane pair	2 and 3
Salt solution	NaCl
Salt ratio (g NaCl in LSS: g NaCl in HSS)	1:15; 1:30; 1:45

2.3 RED tests using feed solutions of different salt pairs

The effect of the feed solution composition on the RED system performance was investigated using NaCl solutions having Li^+, K^+, Ca^{2+}, Mg^{2+} and SO_4^{2-} ions also. The content of different salts in the feed solutions was adjusted as 10 wt% in addition to 90 wt% of NaCl

*Published by Journal of Environmental Chemical Engineering, https://doi.org/10.1016/j.jece.2023.109386

in the mixture. In the meanwhile, the total salt ratio between LSS and HSS was kept constant as 1:30 (g-salt in LSS : g-salt in HSS). These tests were performed with three membrane pairs at three different flow rates. The operational conditions were summarized in Tables 3 and 4.

Table 3. Operational conditions for studies with various salt mixtures

IEMs	CM-AESD and CM-KESD
Numbers of membrane pairs	3
Salt ratio (g NaCl in LSS:g NaCl in HSS)	1:30
Mixtures of salts	NaCl NaCl - LiCl NaCl - KCl NaCl - $MgCl_2$ NaCl - $CaCl_2$ NaCl - Na_2SO_4

Table 4. The amount of salts used in the feed solutions

Chemicals		**NaCl**	**NaCl-LiCl**		**NaCl -KCl**		**NaCl – $CaCl_2$**		**NaCl -$MgCl_2$**		**NaCl - Na_2SO_4**	
			NaCl	**LiCl**	**NaCl**	**KCl**	**NaCl**	**$CaCl_2$**	**NaCl**	**$MgCl_2$**	**NaCl**	**Na_2SO_4**
LSS	**g/L**	1	0.9	0.1	0.9	0.1	0.9	0.13	0.9	0.21	0.9	0.1
	M (mol/L)	0.017	0.015	0.002	0.015	0.0013	0.015	0.0008	0.015	0.001	0.015	0.0007
	N (eq/L)	0.017	0.015	0.002	0.015	0.0013	0.015	0.00016	0.015	0.002	0.015	0.00014
HSS	**g/L**	30	27	3	27	3	27	3	27	3	27	3
	M (mol/L)	0.5	0.46	0.05	0.46	0.05	0.46	0.027	0.46	0.031	0.46	0.021
	N (eq/L)	0.5	0.46	0.05	0.46	0.05	0.46	0.054	0.46	0.062	0.46	0.042

3. Results and discussion

3.1 RED performance of custom-made interpolymer IEMs at different conditions

Monovalent selective IEMs can be synthesized by deposition of very thin layer of polymer with opposite charge or by crosslinking of polyelectrolyte into membrane. Considering the urgent need for specific IEMs with the requested properties for the RED systems, tailor-made membranes based on modified interpolymer of PE and styrene crosslinked with DVB (PE//st-co-DVB) were synthesized and tested in a RED stack. These membranes can be characterized as homogeneous ones. The material studies showed that their structure is like Nafion 117 membranes. They have ionic cluster connected with narrow ionic channels. The dimension of these intercalations depends on the amount of DVB used in the

*Published by Journal of Environmental Chemical Engineering, https://doi.org/10.1016/j.jece.2023.109386

synthesis step. Thus, it is possible to control the membrane morphology and the compactness of the ionic channels. Hence, one can prepare monovalent selective membrane that is desirable for improving the production of energy by the RED stack. The second contribution of interpolymer membranes is a chance to obtain them by extrusion. Hence, such membranes can be prepared by a manufacturer who has access to an extruder. The third feature for processing of interpolymer is an easiness for getting foils with different thickness (the thinner membranes have low resistivity, and they are preferred for RED).

The RED performances of these custom-made interpolymer based IEMs were investigated as a function of membrane pairs number used in the RED stack, feed flow rate, and salt ratio using only NaCl solution. The results of these studies were summarized in Table 5. To understand the relationship between the numbers of membrane pair in the RED stack and the power density generated, the RED stack was prearranged using 2 and 3 pairs of IEMs prepared from custom-made interpolymers. The other investigated parameters were feed flow rates and salt ratio. It is not easy to say that there is a linear relationship between the number of membrane pairs in the RED stack and the power density (Figures 3-5). This may be because of the fact that the resistance of the electrode compartment remains higher than the intracellular stack resistance as a result of the small numbers of membrane pairs [11].

In the studies carried out using feed solutions (LSS and HSS) with a salt ratio of 1:45 (g NaCl in LSS: g NaCl in HSS), the highest power density was obtained with 3 membrane pairs at all flow rates. In addition, it is observed that OCV increased as the numbers of membrane pair increased. The reason why OCV values show a strong relation with increasing number of membrane pairs is that OCV is the sum of the voltage across the stack and each membrane pair added let OCV increase.

The effect of the feed flow rate on the power density was evaluated using both 2 and 3 pairs of IEMs. Figures 6 and 7 show the relationships between the power density and the current density at different flow rates of the feed solutions. Since there was no direct relationship between the flow rates of the feed solutions and power density, it was considered that the flow rate of the feed solutions was not a dominating factor of the RED process. Maybe the reason for the independence of power density from the feed flow rate was the relatively large inter-membrane distance (400 μm) when especially the proportion of LSS resistance in the stack is high.

In order to investigate the effect of the salinity gradient on the power generation, salt concentration in HSS was altered as 15, 30 and 45 g/L while the salt concentration of LSS

was kept constant as 1 g/L. As depicted in Figures 8 and 9, the power density increased with the increasing salt concentration in HSS for both 2 and 3 membrane pairs. This result might stem from the increasing salinity gradient as the main driving force in RED process. In addition, OCV increased also by the increase in the salt concentration difference between LSS and HSS.

Table 5. The values of OCV, maximum power density obtained by RED tests at different conditions

Number of membrane pair	Salt ratio (g NaCl in LSS : g NaCl in HSS)	Feed flow rate (mL/min)	OCV (V)	Maximum power density (W/m^2)
2	1:15	20	0.173	0.132
		40	0.236	0.180
		60	0.236	0.172
		80	0.237	0.188
	1:30	20	0.280	0.283
		40	0.288	0.313
		60	0.291	0.351
		80	0.292	0.301
	1:45	20	0.276	0.405
		40	0.317	0.343
		60	0.316	0.329
		80	0.311	0.315
3	1:15	30	0.302	0.168
		60	0.358	0.175
		90	0.356	0.164
		120	0.356	0.163
	1:30	30	0.427	0.305
		60	0.431	0.278
		90	0.435	0.270
		120	0.435	0.256
	1:45	30	0.469	0.528
		60	0.480	0.529
		90	0.483	0.531
		120	0.486	0.561

*Published by Journal of Environmental Chemical Engineering, https://doi.org/10.1016/j.jece.2023.109386

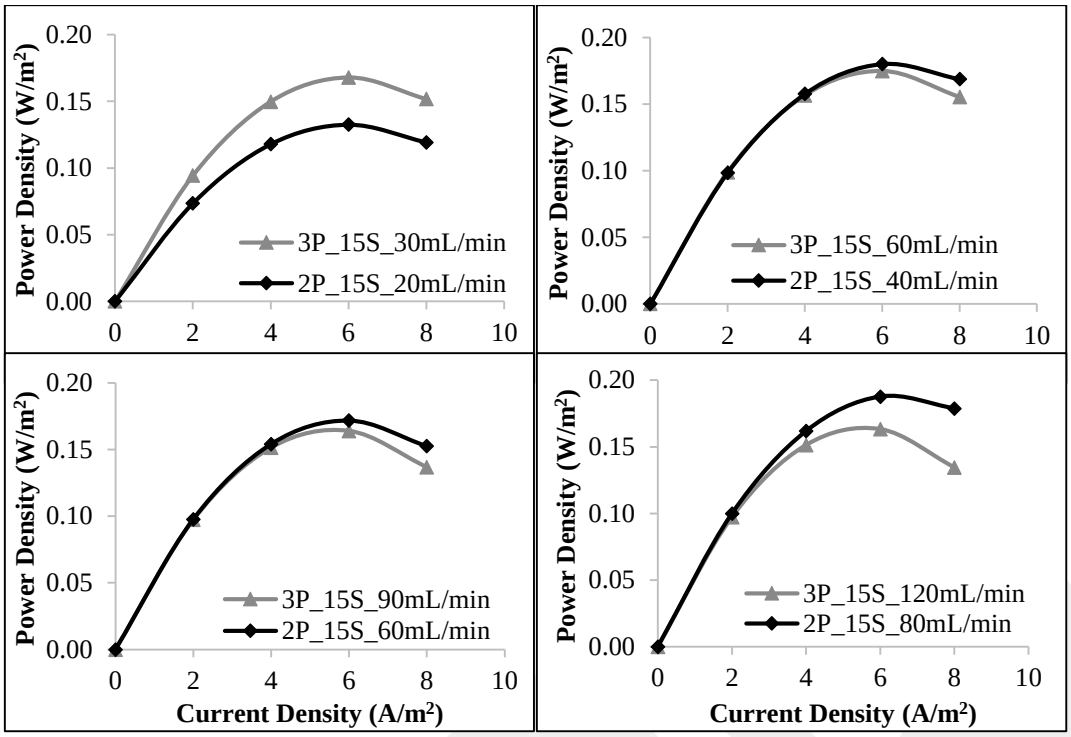

Figure 3. Power density vs. current density plots for the salinity ratio of 1:15 as a function of membrane pair number (P: number of membrane pairs 15S: salt ratio (1 g/L NaCl in LSS and 15 g/L NaCl in HSS)

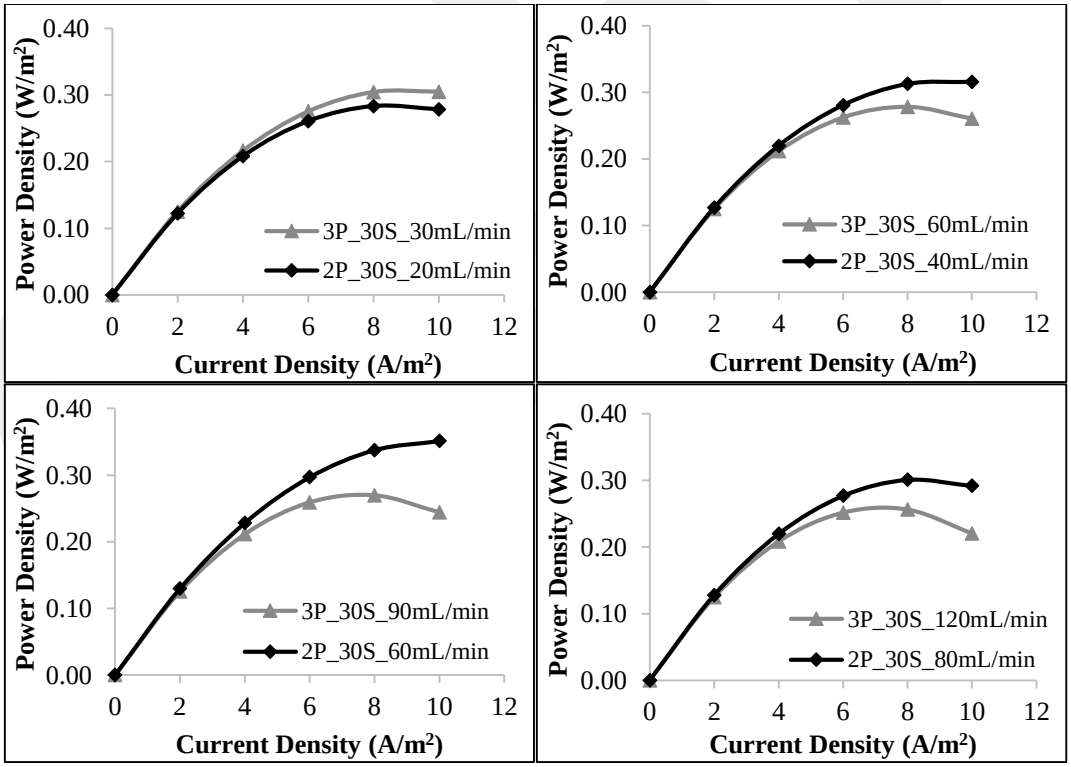

Figure 4. Power density vs. current density plots for the salinity ratio of 1:30 as a function of membrane pair number (P: number of membrane pairs 30S: salt ratio (1 g/L NaCl in LSS and 30 g/L NaCl in HSS)

*Published by Journal of Environmental Chemical Engineering, https://doi.org/10.1016/j.jece.2023.109386

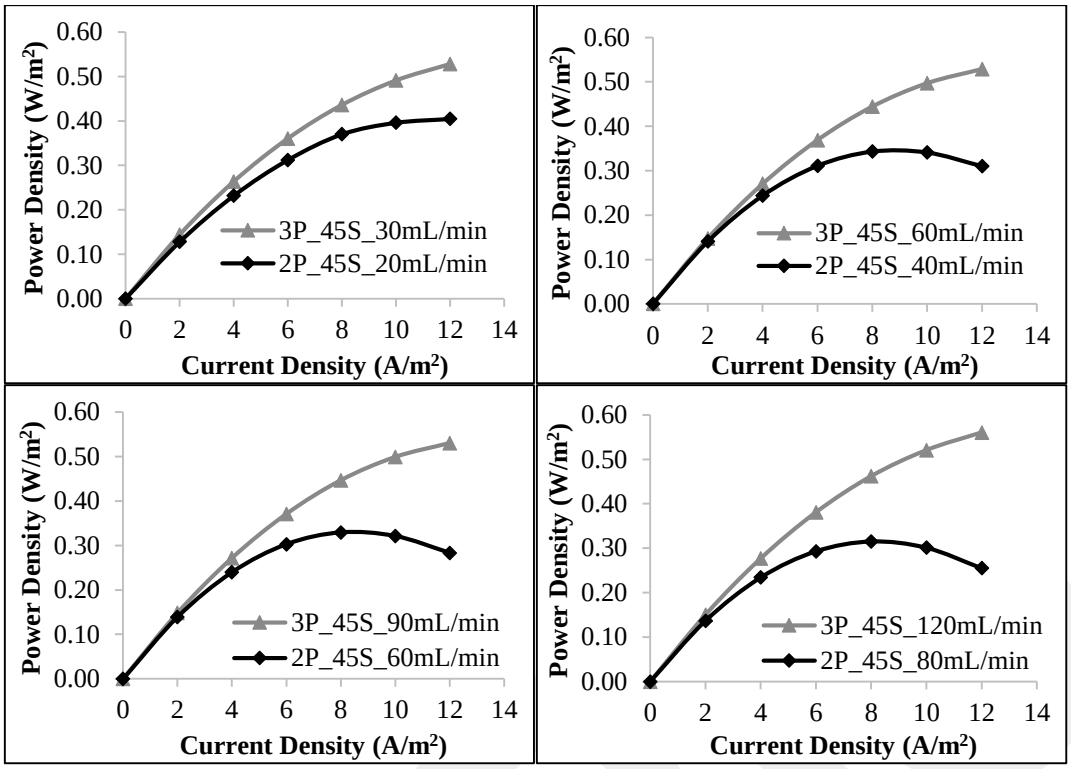

Figure 5. Power density vs. current density plots for the salinity ratio of 1:45 as a function of membrane pair number (P: number of membrane pairs 45S: salt ratio (1 g/L NaCl in LSS and 45 g/L NaCl in HSS)

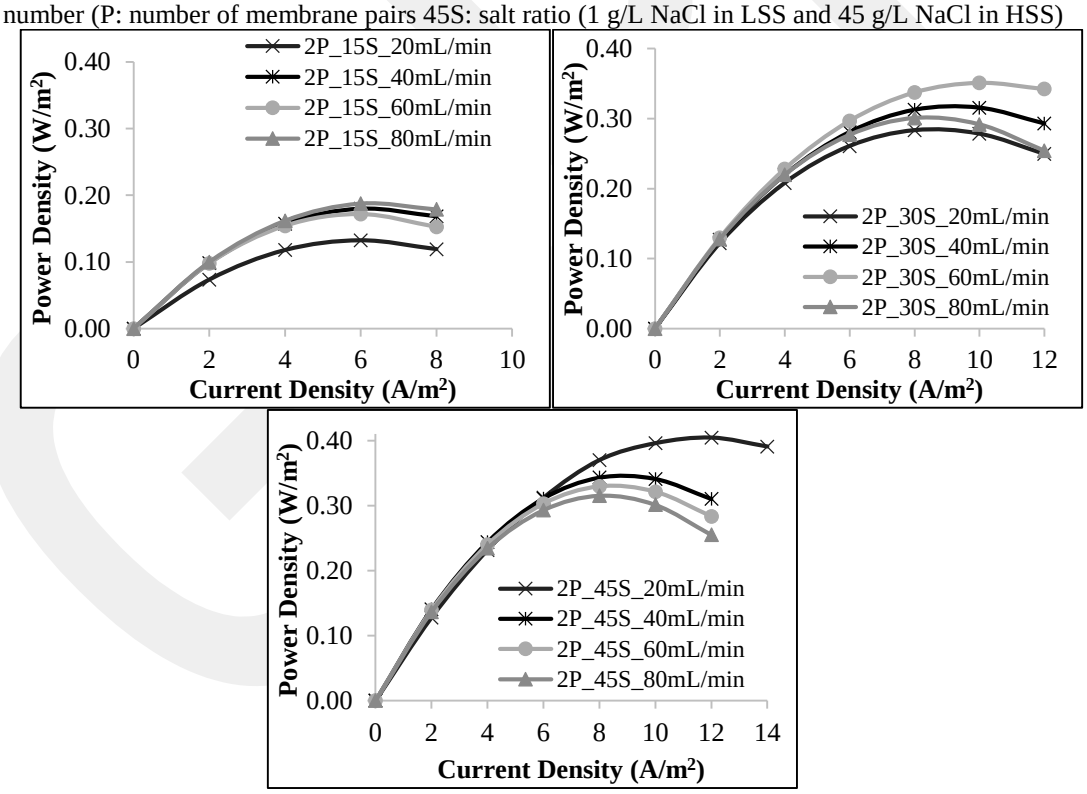

Figure 6. Power density vs. current density plots for various salinity ratios as a function of flow rate of feed solutions (Number of membrane pairs (P):2; salt ratios (1 g/L NaCl in LSS and 15, 30, 45 g/L NaCl in HSS)

*Published by Journal of Environmental Chemical Engineering, https://doi.org/10.1016/j.jece.2023.109386

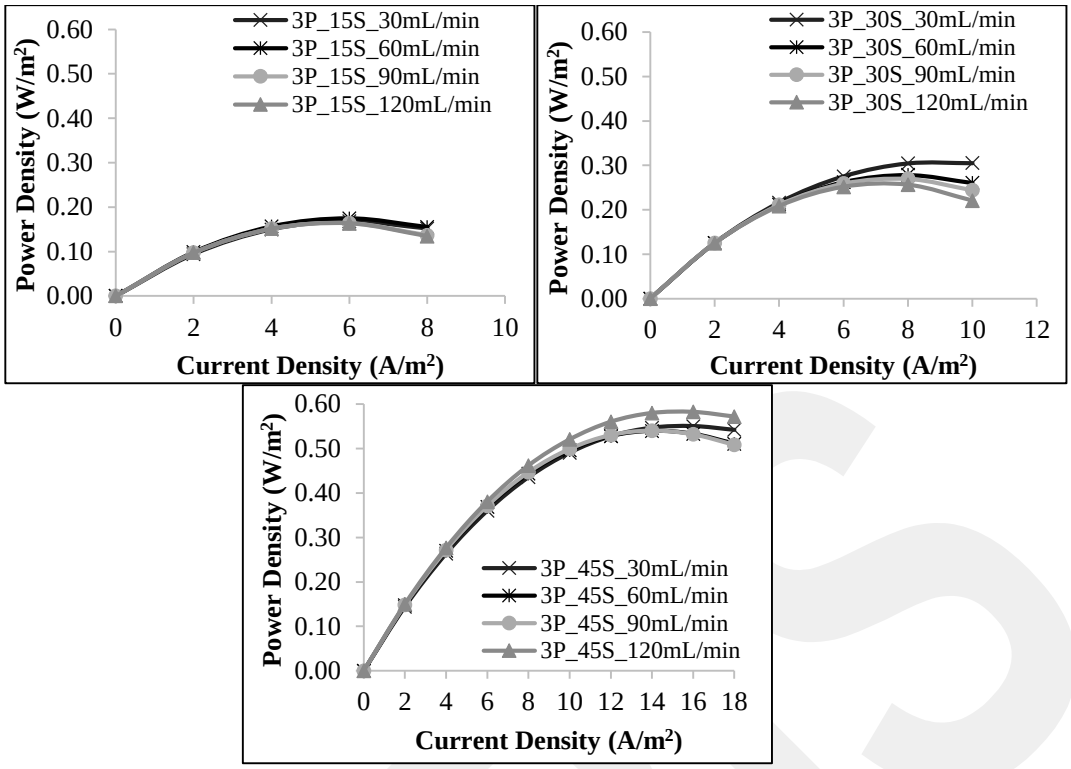

Figure 7. Power density vs. current density plots for various salinity ratios as a function of flow rate of feed solutions (Number of membrane pairs (P):3; salt ratios (1 g/L NaCl in LSS and 15, 30, 45 g/L NaCl in HSS)

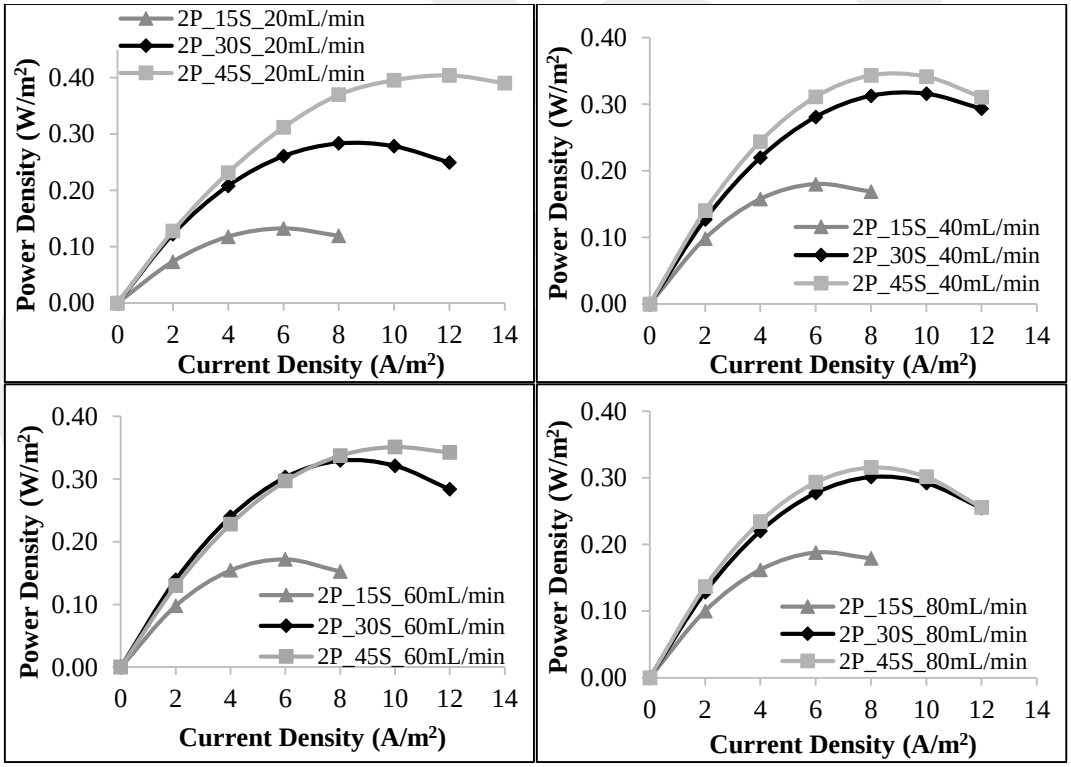

Figure 8. Power density vs. current density plots as a function of salinity gradient (Number of membrane pairs (P):2; salt ratios (1 g/L NaCl in LSS and 15, 30, 45 g/L NaCl in HSS)

*Published by Journal of Environmental Chemical Engineering, https://doi.org/10.1016/j.jece.2023.109386

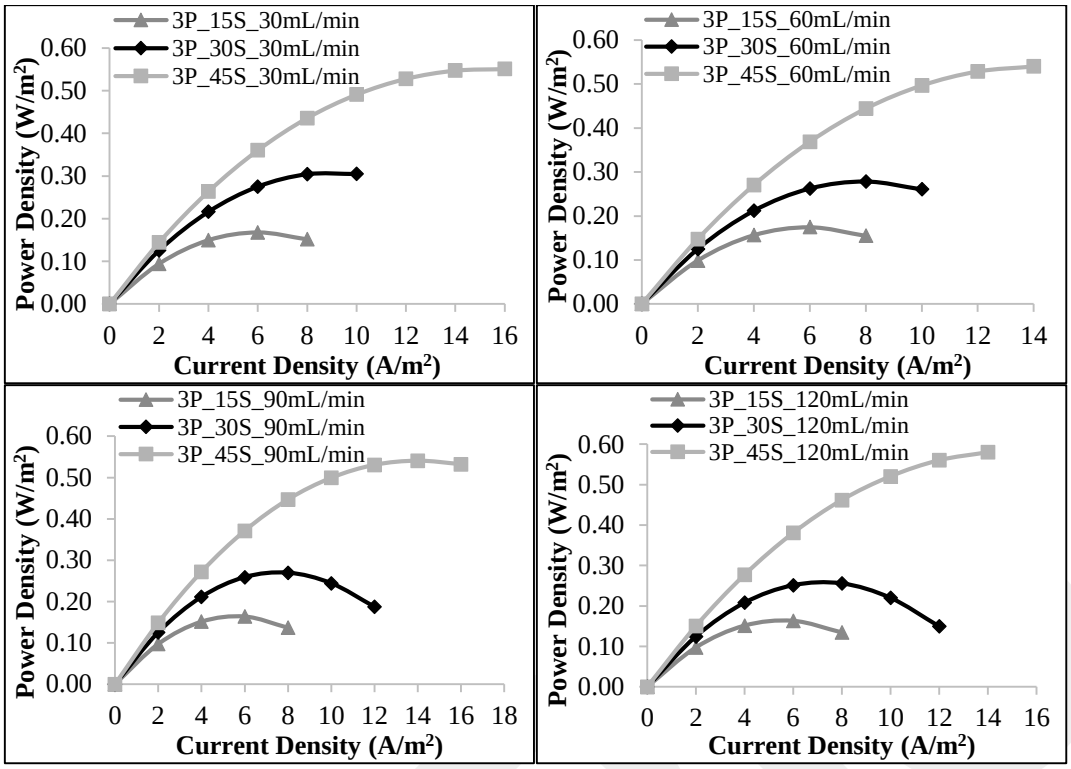

Figure 9. Power density vs. current density plots as a function of salinity gradient
(Number of membrane pairs (P): 3; salt ratios (1 g/L NaCl in LSS and 15, 30, 45 g/L NaCl in HSS)

The performances of the custom-made interpolymer IEMs were summarized and compared with those of commercial IEMs in Table 6. The custom-made IEMs have properties in the range of properties of some commercial IEMs and the power density obtained from the stack equipped with these membranes does not differ significantly from the Fuji IEMs.

Table 6. Comparison of power density obtained from the RED stack equipped with selected membrane systems.

Membrane*	Resistance (Ohm cm^2)	Ion exchange capacity (mmol/g)	IEM structure	Power density** (W/m^2)	Reference
Neosepta CMX	1.67	2.30	Homogeneous	0.56	[29]
Neosepta AMX	2.91	1.62	Homogeneous		
FumaTech CEM	2.14	1.14	Homogeneous	1.20	[30]
FumaTech AEM	1.03	1.12	Homogeneous		
Fuji CEM	2.97	1.10	Homogeneous	0.29	[11]
Fuji AEM	1.55	1.40	Homogeneous		
Ralex CMH	11.33	2.34	Heterogeneous	0.60	[11]
Ralex AMH	7.66	1.97	Heterogeneous		
CEM-KESD	4.22	1.03	Homogeneous	0.30	This study
AEM-AESD	0.95	0.80	Homogeneous		

*The thicknesses of the IEMs are in the range of 100-200 micrometer (except Ralex membranes with the thickness > 400 micrometer).
**Salt ratio is 1:30 (salt concentration in LSS: salt concentration in HSS)

*Published by Journal of Environmental Chemical Engineering, https://doi.org/10.1016/j.jece.2023.109386

When we compared the power density values for a different set of membranes, FumaTech membranes was recognized to be the most efficient membranes. Such result was related neither to the membrane thickness (all homogenous membranes were 100-200 micrometers thick) nor to the contents of ionogenic groups (pretty similar values of ion exchange capacity –except Neosepta membranes). The energy harvesting in the salinity gradient system by interpolymer membranes did not exceed the performance of other membranes. It offered value comparable to Fuji membranes, despite interpolymer membranes having a lower concentration of ionogenic groups (thus a higher resistance). Hence, it could be expected that the recovery of energy from the salinity gradient by the RED system relies mostly on the membrane structure and can be affected by membrane thickness, membrane permselecivity, and membrane ion-exchange capacity. The other parameters, like stack geometry, the distance between membranes, feed composition, or flow rate, should be considered also. The same of them are discussed in this paper.

3.2 Effect of different co-existing ions of RED performance of custom-made interpolymer IEMs

The effect of co-existing ions on RED performance was investigated by using 3 pairs of custom-made interpolymer membranes CM-AESD and CM-KESD and 1:30 of the salt ratio. Initially, the feed solutions were prepared by using only NaCl. Figure 10(a) shows that the maximum power density was obtained as 0.309 W/m^2 at the highest feed flow rate of 120 mL/min. The effect of feed flow rate on power generation by the RED system cannot be explained clearly in the literature. Thus, the optimum feed flow rate should be determined by obtaining the maximum power density [11]. The feed flow rate which is higher than optimum one can result in (1) insufficient time for migration of ions (2) high pressure losses (3) lower voltage and power output. If the feed flow rate increases up to an optimum value, some improvements may be achieved such as (1) reduction of concentration polarization (2) enhancement of hydrodynamic mixing (3) higher voltage and power output.

The effect of Li^+ ions co-existing in the feed solutions of NaCl on power generation by RED was investigated by using 3 pairs of CM-AESD and CM-KESD membranes. During the RED tests, the content of LiCl was adjusted as 10 wt% in HSS and LSS. The power density increased with an increase in the flow rate of feed solutions and the maximum power density was obtained as 0.270 W/m^2 at 120 mL/min (Figure 10(b)).

As mentioned before, the maximum power density was 0.309 W/m^2 in the run with NaCl solutions only. However, when the feed solutions having LiCl along with NaCl were used in the RED tests, the maximum power density reduced to 0.270 W/m^2.

The ionic radius and diffusion coefficients of various ions are given in Table 7. The ionic mobilities are related with these properties. When the ionic mobilities of Na^+ and Li^+ ions are compared, Li^+ ions are slower than Na^+ ions. In fact, Li^+ ion has larger hydrated radius (3.82 Å) and thus lower diffusion coefficient ($1.029x10^{-5}$ cm/s) than that of Na^+ ion (3.58 Å and $1.334x10^{-5}$ cm/s). The Li^+ ions were exposed to a higher membrane resistance because of its larger hydrated radius, thus the transport of Li^+ ions through the CEMs will be restricted. Because of the weaker ionic transport of Li^+ ions through CEMs, the power density was reduced from 0.309 W/m^2 to 0.270 W/m^2 with the addition of LiCl salt to the feed solution containing NaCl. It was concluded that the Li^+ ion has a diminishing effect on the power density generated. The feed solutions were also prepared by adding 10 wt% KCl in the LSS and HSS having 90 wt% NaCl. As seen in Figure 10(c), the maximum power density achieved was 0.398 W/m^2. This value was greater than the result of the RED test performed with only NaCl solutions (0.309 W/m^2). The hydrated radius of K^+ ion is smaller (3.31 Å) than that of Na^+ ion (3.58 Å). In the transport of ions through IEMs, the mobility of ions having larger hydrated radius is slower than the smaller ones. Thus, K^+ ion has a higher ionic mobility and diffusion coefficient than those of Na^+ ion. Therefore, transfer of K^+ ions through CEMs becomes easier and faster than that of Na^+ ions. It is considered that the internal resistances of CEMs should be lower in the presence of K^+ ions.

Table 7. Hydrated radius and diffusion coefficient of co-existing ions

Ions	**Hydrated radius (Å) [31]**	**Diffusion coefficient ($x10^{-5}$ cm/s) [22, 32]**
Na^+	3.58	1.334
Li^+	3.82	1.029
K^+	3.31	1.957
Ca^{2+}	4.12	0.792
Mg^{2+}	4.28	0.706
SO_4^{2-}	3.79	1.065
Cl^-	3.32	2.032

Each divalent cation (Mg^{2+} or Ca^{2+}) is exchanged with two monovalent cations (Na^+) through the CEMs for providing the electroneutrality on the membrane sides. This kind of transportation is called uphill transport which means that the transport of ions against the concentration gradient [22, 24, 31, 32]. During the transport of Ca^{2+} ions, the multivalent ions caused an increase in ohmic drop and the electrical resistance of the RED stack increased [24]. In addition to this, the electrical resistance of CEMs has risen and the lower

electromotive force was obtained by the addition of the divalent cations (Mg^{2+} and Ca^{2+}) due to their low mobilities as divalent ions within the membranes. Because of having lower ionic mobility and higher hydrated radius of the divalent ions, the diffusions of multivalent ions are slower. Moreno et al. [33] stated that the stack resistance will be higher and stronger in the presence of Mg^{2+} and Ca^{2+} ions in the feed solutions. There are other reasons for the observed phenomenon such as (1) high valence in divalent counter ions, (2) high affinity between divalent ions and fixed functional groups in IEMs, (3) lower activity coefficients of divalent ions than those of monovalent ions, and (4) higher hydrated radius of divalent ions than those of monovalent ions [24, 34, 35]. Depending on these properties, the obtained OCV values decreased and therefore the lower power was generated in the RED stack [22]. In our case, when our OCV results were examined, we did not observe so dramatic alteration of OCV values with the addition of monovalent and multivalent ions to the feed solutions at different flow rates. On the other hand, the power density results obtained by the addition of divalent ions (Mg^{2+}, Ca^{2+} and SO_4^{2-}) to the feed solutions were found to be lower than that of the study performed with the feed solutions containing only NaCl.

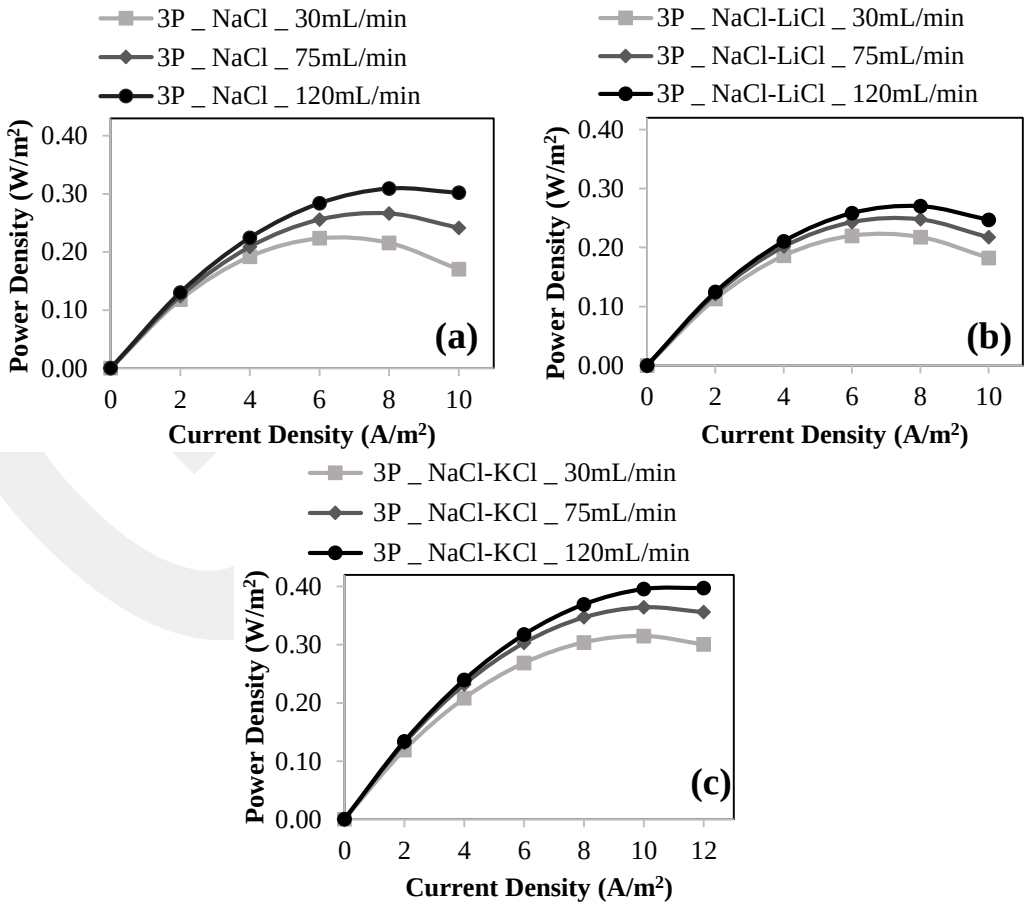

*Published by Journal of Environmental Chemical Engineering, https://doi.org/10.1016/j.jece.2023.109386

Figure 10. Power density vs. current density plots obtained with (a) only NaCl solutions (b) mixtures of NaCl and LiCl solutions (c) mixtures of NaCl and KCl solutions

In order to observe the effect of divalent ions on the RED performance of tailor-made interpolymer IEMs, feed solutions were prepared using 10 wt% of $CaCl_2$ and 90 wt% NaCl in the mixture. The feed flow rate was almost ineffective on the power density. The maximum power density was reduced to 0.297 W/m^2 in the presence of Ca^{2+} ions having a larger hydrated radius than Na^+ ions (Figure 11(a)). Next studies were performed using $MgCl_2$ by using 10 wt% of $MgCl_2$ and 90 wt% of NaCl. The power density results obtained were very close to each other as 0.285, 0.300, and 0.299 W/m^2 at the feed flow rates of 30, 75, and 120 mL/min (Figure 11(b)). When the data obtained were compared to those with feed solutions containing only NaCl, it was seen that Mg^{2+} ion with a larger hydrated radius and a lower diffusion coefficient than Na^+ ion caused some reduction in the power density.

Pintossi et al. [24] investigated the effect of SO_4^{2-} ions on power density and explained that the presence of SO_4^{2-} ions resulted in the loss of permselectivity of membrane having a high swelling degree. This explanation has been supported by the measurements of the membrane permselectivity in a mixture having both NaCl and Na_2SO_4. It was concluded that increasing portion of SO_4^{2-} ions up to 50 wt% in the mixture caused a certain decrease in power generation during RED tests using Fujifilm type 1, Fujifilm type 10, Neosepta AMX, and monovalent ion selective Neosepta ACS membranes [24]. Similar explanations were made by Rijnaarts et al. [25] and Moreno et al. [33]. The lower permselectivity results in higher electrical resistance of the AEMs. This situation is like the increase in the electrical resistances of the CEMs in the presence of multivalent cations [26].

In our study, the effect of SO_4^{2-} ions on power density was investigated using the feed solutions prepared with 10 wt% of Na_2SO_4 and 90 wt% of NaCl. The maximum power density was found as 0.246 W/m^2 at the lowest flow rate of 30 mL/min (Figure 11(c)). The generated power density and the OCV values were lower than those of the power density obtained with the feed solutions having only NaCl. The reason is that the hydrated radius of Cl^- ions is smaller than the hydrated radius of SO_4^{2-} ions. So, the transfer of Cl^- ions through AEMs was easier than that of SO_4^{2-} ions. Consequently, the power density has been found higher by using the feed solutions prepared with only NaCl.

*Published by Journal of Environmental Chemical Engineering, https://doi.org/10.1016/j.jece.2023.109386

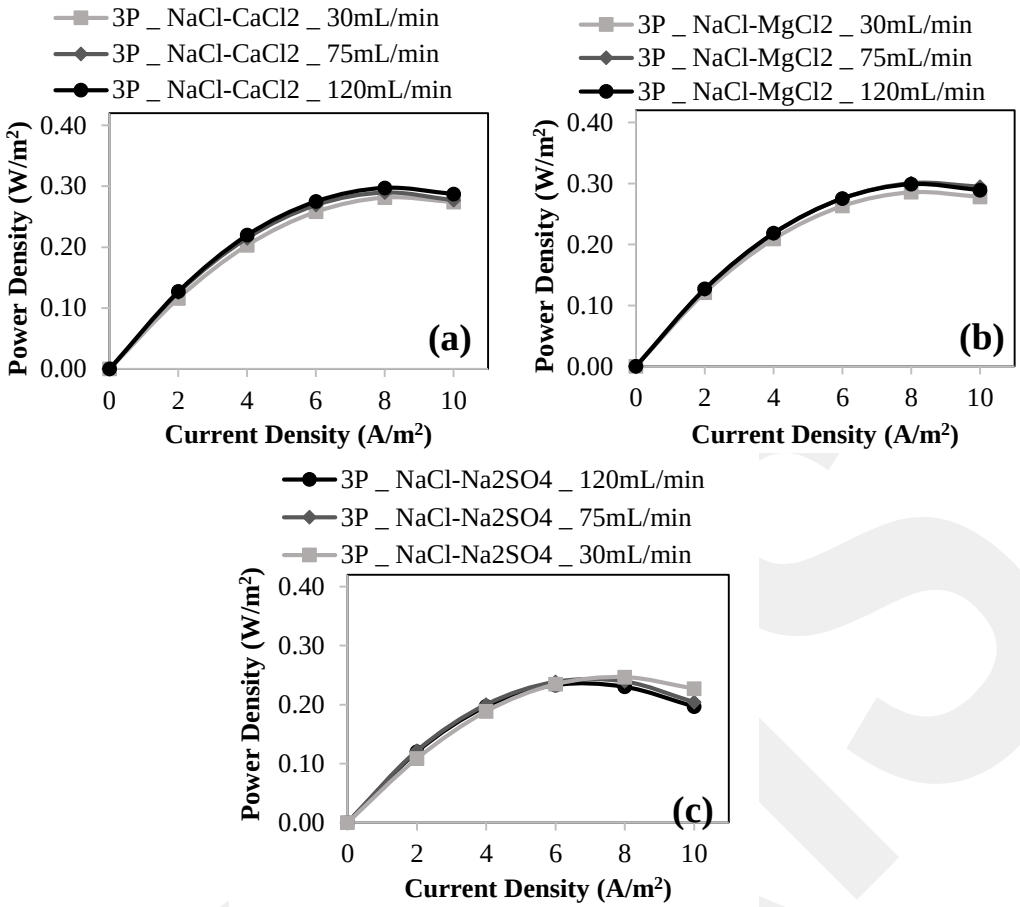

Figure 11. Power density results of experiments where feed is mixture of (a) NaCl and $CaCl_2$ solutions (b) NaCl and $MgCl_2$ solutions (c) NaCl and Na_2SO_4 solutions

The overall experimental results of the effects of co-existing ions are shown in Table 8. In the presence of monovalent ions, the lowest power generation was obtained by using the feed solutions containing both NaCl and LiCl because of larger hydrated radius and smaller diffusion coefficient of Li^+ ion than those of Na^+ and K^+ ions. On the other hand, because of the valence, the higher affinity of divalent ions (Mg^{2+}, Ca^{2+}, and SO_4^{2-}) to the fixed functional groups than that of monovalent ions (Na^+, Li^+, K^+, and Cl^-) limited the diffusion of divalent ions in the membrane and reduced the power generation performance of the RED system [36]. In the presence of divalent ions, the strong affinity of divalent ions by IEMs may cause an increase in the membrane resistance. A high membrane resistance reduced the performance of the RED system for power generation. When all results are compared, it is seen that the lowest and highest power density values obtained were 0.246 W/m^2 at 30 mL/min in the presence of SO_4^{2-} ions and 0.398 W/m^2 at 120 mL/min in the presence of K^+ ions, respectively.

*Published by Journal of Environmental Chemical Engineering, https://doi.org/10.1016/j.jece.2023.109386

The OCV gives the maximum power generation potential of the RED stack and it is obtained experimentally at zero current. The OCV is defined as the difference of voltage, arising from the salinity gradient between LSS and HSS [37, 38]. Hossen et al. [37] modified the Nernst equation by the replacement of the activity coefficients with the conductivities of LSS and HSS. In all studies, the salt ratio of two feed solutions was kept constant at 1:30 (g-salt in LSS/g-salt in HSS), therefore, the conductivities of feed solutions did not change. It was seen that there was no significant effect of the presence of co-existing ions in the feed solutions on OCV values (Table 8). The maximum OCV value obtained in the study performed with feed solutions including only NaCl was 0.445 V at 120 mL/min. This value became 0.444 V by the addition of 10 wt% KCl to the feed solutions with almost no change. The maximum OCV value was around 0.430 V in the presence of LiCl, $MgCl_2$, $CaCl_2$, and Na_2SO_4 in the feed solutions together with NaCl.

Guo et al. [23] stated that the OCV value highly depends on the valence of ions in the feed solutions. The multivalent ions are reported to give a lower OCV value than those of monovalent ions. In this work, the lower OCV value was obtained by the addition of $MgCl_2$, $CaCl_2$ and Na_2SO_4 salts to the feed solution containing NaCl. According to the Nernst equation used for calculation of OCV, a very small decrease in OCV is obtained with a mixture containing KCl and NaCl. As the activity coefficient of KCl is lower than that of NaCl, replacement of 10 wt% of NaCl with 10 wt% of KCl caused a slight decrease in OCV value.

*Published by Journal of Environmental Chemical Engineering, https://doi.org/10.1016/j.jece.2023.109386

Table 8. Performance of custom-made interpolymer IEMs for different salt mixtures

Number of membrane pairs	Feed solutions	Feed flow rate (mL/min)	Maximum power density (W/m^2)	Open circuit voltage (V)
3	NaCl	30	0.224	0.418
		75	0.294	0.429
		120	0.309	0.445
	NaCl-LiCl	30	0.220	0.392
		75	0.248	0.424
		120	0.270	0.432
	NaCl-KCl	30	0.315	0.404
		75	0.364	0.436
		120	0.398	0.444
	NaCl-$CaCl_2$	30	0.281	0.378
		75	0.289	0.428
		120	0.297	0.431
	NaCl-$MgCl_2$	30	0.285	0.406
		75	0.300	0.429
		120	0.299	0.432
	NaCl-Na_2SO_4	30	0.246	0.350
		75	0.239	0.425
		120	0.233	0.423

4. Conclusions

The custom-made interpolymer IEMs synthesized were successfully employed for salinity gradient energy production by RED. The use of homemade IEMs extends significantly the classes of materials to be applied in the RED stack. According to literature [27], the used interpolymer of PE/St/DVB= 68/20/2 has a homogeneous structure with aromatic components organized in 5 nm clusters connected with 1 nm channels. After chemical modification, these features turned into polyelectrolytes that controlled the transport of ions. Such kinds of membranes can be produced by any polymer manufacturer that has an extruder.

The highest power density value was 0.561 W/m^2 obtained with three membrane pairs and 120 mL/min of the feed flow rate by using only NaCl solutions with 1:45 of the salt ratio (g NaCl in LSS: g NaCl in HSS). As anticipated by the Nernst equation, which states that the electrical potential is proportional to the salinity gradient (i.e. salt ratio of feed solutions), it was discovered that the maximum power densities could be obtained when the salinity gradient is high. The presence of the co-existing ions had a slight impact on OCV values. Due to low hydrated radius and high diffusion coefficient, monovalent ions with high ionic

*Published by Journal of Environmental Chemical Engineering, https://doi.org/10.1016/j.jece.2023.109386

mobility are easily transported via IEMs. Therefore, the RED system may generate more power because monovalent ions are exposed to comparatively lower membrane resistance than divalent ions. The maximum power density was obtained by the addition of K^+ ions to the feed solutions. On the other hand, the addition of SO_4^{2-} ions decreased the membrane permselectivity and increased the resistance of AEMs. This situation was like the behavior of the CEMs in the presence of multivalent cations such as Ca^{2+} and Mg^{2+} ions.

Author Contributions: Conceptualization, E.A. and T.Z.K.; Methodology, E.A. and T.Z.K.; Membrane synthesis, K.S.K. and M.B.; Writing – Original Draft Preparation, E.A., T.Z.K. and E.G., Writing – Review & Editing, E.G., N.K., M.B., and B.T.; Supervision, E.G., M.B., and N.K.; Project Administration, N.K., M.B., B.T.; Funding Acquisition, N.K., M.B. All authors have read and agreed to the published version of the manuscript.

Funding: This research was funded by TÜBİTAK, grant number TÜBİTAK 117M023.

Acknowledgement: This research has been financially supported by the bilateral collaboration programme (TUBITAK-NCBR-2549) between Turkey and Poland (Project No: TÜBİTAK 117M023). E. Altıok is grateful for the PhD scholarship of Turkish Higher Education Council (YÖK 100-2000).

Conflicts of interest: The authors declare no conflict of interest.

*Published by Journal of Environmental Chemical Engineering, https://doi.org/10.1016/j.jece.2023.109386

REFERENCES

[1] Yip, N. Y., Brogioli, D., Hamelers, H. V., Nijmeijer, K. (2016). Salinity gradients for sustainable energy: primer, progress, and prospects. Environmental Science and Technology, 50(22), 12072-12094.

[2] Alvarez-Silva, O., Winter, C., Osorio, A. F. (2014). Salinity gradient energy at river mouths. Environmental Science and Technology Letters, 1(10), 410-415.

[3] Alvarez-Silva, O., & Osorio, A. F. (2015). Salinity gradient energy potential in Colombia considering site specific constraints. Renewable Energy, 74, 737-748.

[4] Zhao, T., Xu, M., Xiao, X., Ma, Y., Li, Z., & Wang, Z. L. (2021). Recent progress in blue energy harvesting for powering distributed sensors in ocean. Nano Energy, 88, 106199.

[5] Fortunato, J., Peña, J., Benkaddour, S., Zhang, H., Huang, J., Zhu, M., Logan, B. E., & Gorski, C. A. (2020). Surveying manganese oxides as electrode materials for harnessing salinity gradient energy. Environmental Science and Technology, 54(9), 5746-5754.

[6] Burheim, O. S., Liu, F., Sales, B. B., Schaetzle, O., Buisman, C. J., & Hamelers, H. V. (2012). Faster time response by the use of wire electrodes in capacitive salinity gradient energy systems. The Journal of Physical Chemistry C, 116(36), 19203-19210.

[7] Lin, S., Straub, A. P., Elimelech, M. (2014). Thermodynamic limits of extractable energy by pressure retarded osmosis. Energy and Environmental Science, 7(8), 2706-2714.

[8] La Mantia, F., Pasta, M., Deshazer, H. D., Logan, B. E., Cui, Y. (2011). Batteries for efficient energy extraction from a water salinity difference. Nano Letters, 11(4), 1810-1813.

[9] Shaposhnik, V. A., Kesore, K. (1997). An early history of electrodialysis with permselective membranes. Journal of Membrane Science, 136(1-2), 35-39.

[10] Siekierka, A., Smolińska-Kempisty, K., Bryjak, M. (2020). Charge-doped electrodes for power production using the salinity gradient in CapMix. Desalination, 495, 114670.

[11] Altıok, E., Kaya, T. Z., Güler, E., Kabay, N., Bryjak, M. (2021). Performance of reverse electrodialysis system for salinity gradient energy generation by using a commercial ion exchange membrane pair with homogeneous bulk structure. Water, 13(6), 814.

[12] Pattle, R. E. (1954). Production of electric power by mixing fresh and salt water in the hydroelectric pile. Nature, 174(4431), 660-660.

[13] Kang, H., Kim, E., Jung, S. P. (2017). Influence of flow rates to a reverse electro-dialysis (RED) stack on performance and electrochemistry of a microbial reverse electrodialysis cell (MRC). International Journal of Hydrogen Energy, 42(45), 27685-27692.

*Published by Journal of Environmental Chemical Engineering, https://doi.org/10.1016/j.jece.2023.109386

[14] Tedesco, M., Brauns, E., Cipollina, A., Micale, G., Modica, P., Russo, G., Helsen, J. (2015). Reverse electrodialysis with saline waters and concentrated brines: a laboratory investigation towards technology scale-up. Journal of Membrane Science, 492, 9-20.

[15] Lacey, R. E. (1980). Energy by reverse electrodialysis. Ocean Engineering, 7(1), 1-47.

[16] Wilcox, J. (2014). Grand challenges in advanced fossil fuel technologies. Frontiers in Energy Research, 2, 47.

[17] Zoungrana, A., Çakmakci, M. (2021). Optimization of the reverse electrodialysis power output through the ratio of the feed solutions salinity. IET Renewable Power Generation, 15(4), 769-777.

[18] Guler, E., & Nijmeijer, K. (2018). Reverse electrodialysis for salinity gradient power generation: Challenges and future perspectives. Journal of Membrane Science and Research, 4(3), 108-110.

[19] Abidin, M. N. Z., Nasef, M. M., & Veerman, J. (2022). Towards the development of new generation of ion exchange membranes for reverse electrodialysis: A review. Desalination, 537, 115854.

[20] Mei, Y., Tang, Ch.Y. (2018). Recent developments and future perspectives of reverse electrodialysis technology: A review. Desalination, 425, 156–174.

[21] Gomez-Coma, L., Ortiz-Martinez, V., Carmona, J., Palacio, L., Pradanos, P., Fallanza, M., Ortiz, A., Ibanez, R., Ortiz, I. (2019). Modeling the influence of divalent ions on membrane resistance and electric power in reverse electrodialysis. Journal of Membrane Science, 592, 117385.

[22] Vermaas, D. A., Veerman, J., Saakes, M., & Nijmeijer, K. (2014). Influence of multivalent ions on renewable energy generation in reverse electrodialysis. Energy and Environmental Science, 7(4), 1434-1445.

[23] Guo, Z. Y., Ji, Z. Y., Zhang, Y. G., Yang, F. J., Liu, J., Zhao, Y. Y., Yuan, J. S. (2018). Effect of ions (K^+, Mg^{2+}, Ca^{2+} and SO_4^{2-}) and temperature on energy generation performance of reverse electrodialysis stack. Electrochimica Acta, 290, 282-290.

[24] Pintossi, D. (2021). Fouling in reverse electrodialysis: monitoring, modeling, and control, Ph.D. Thesis, Technische Universiteit Eindhoven, Eindhoven, The Netherlands, 2009.

*Published by Journal of Environmental Chemical Engineering, https://doi.org/10.1016/j.jece.2023.109386

[25] Rijnaarts, T., Huerta, E., van Baak, W., Nijmeijer, K. (2017). Effect of divalent cations on RED performance and cation exchange membrane selection to enhance power densities. Environmental Science and Technology, 51(21), 13028-13035.

[26] Oh, Y., Jeong, Y., Han, S. J., Kim, C. S., Kim, H., Han, J. H., Hwang, K. S., Jeong, N. J., Park, J. S., Chae, S. (2018). Effects of divalent cations on electrical membrane resistance in reverse electrodialysis for salinity power generation. Industrial and Engineering Chemistry Research, 57(46), 15803-15810.

[27] Smolinska-Kempisty, K., Siekierka, A., Bryjak, M. (2020). Interpolymer ion exchange membranes for CapMix process. Desalination, 482, 114384.

[28] Długołęcki, P., Ogonowski, P., Metz, S. J., Saakes, M., Nijmeijer, K., & Wessling, M. (2010). On the resistances of membrane, diffusion boundary layer and double layer in ion exchange membrane transport. Journal of Membrane Science, 349(1-2), 369-379.

[29] Długołęcki, P., Gambier, A., Nijmeijer, K., & Wessling, M. (2009). Practical potential of reverse electrodialysis as process for sustainable energy generation. Environmental Science & Technology, 43(17), 6888-6894.

[30] Vermaas, D. A., Saakes, M., & Nijmeijer, K. (2011). Doubled power density from salinity gradients at reduced intermembrane distance. Environmental Science & Technology, 45(16), 7089-7095.

[31] Hong, J. G., Zhang, W., Luo, J., Chen, Y. (2013). Modeling of power generation from the mixing of simulated saline and freshwater with a reverse electrodialysis system: The effect of monovalent and multivalent ions. Applied Energy, 110, 244-251.

[32] Post, J. W., Hamelers, H. V., Buisman, C. J. (2009). Influence of multivalent ions on power production from mixing salt and fresh water with a reverse electrodialysis system. Journal of Membrane Science, 330(1-2), 65-72.

[33] Moreno, J., Díez, V., Saakes, M., Nijmeijer, K. (2018). Mitigation of the effects of multivalent ion transport in reverse electrodialysis. Journal of Membrane Science, 550, 155-162.

[34] Samson, E., Marchand, J., & Snyder, K. A. (2003). Calculation of ionic diffusion coefficients on the basis of migration test results. Materials and Structures, 36(3), 156-165.

[35] Jang, J., Kang, Y., Han, J. H., Jang, K., Kim, C. M., Kim, I. S. (2020). Developments and future prospects of reverse electrodialysis for salinity gradient power generation: Influence of ion exchange membranes and electrodes. Desalination, 491, 114540.

*Published by Journal of Environmental Chemical Engineering, https://doi.org/10.1016/j.jece.2023.109386

[36] Galizia, M., Benedetti, F. M., Paul, D. R., & Freeman, B. D. (2017). Monovalent and divalent ion sorption in a cation exchange membrane based on cross-linked poly (p-styrene sulfonate-co-divinylbenzene). Journal of Membrane Science, 535, 132-142.

[37] Hossen, E. H., Gobetz, Z. E., Kingsbury, R. S., Liu, F., Palko, H. C., Dubbs, L. L., Coronell, O., Call, D. F. (2020). Temporal variation of power production via reverse electrodialysis using coastal North Carolina waters and its correlation to temperature and conductivity. Desalination, 491, 114562.

[38] Tedesco, M., Scalici, C., Vaccari, D., Cipollina, A., Tamburini, A., Micale, G. (2016). Performance of the first reverse electrodialysis pilot plant for power production from saline waters and concentrated brines. Journal of Membrane Science, 500, 33-45.

*Published by Journal of Environmental Chemical Engineering, https://doi.org/10.1016/j.jece.2023.109386